Determination of the $^{9}Be(\alpha,n)^{12}C$ reaction rate

R. Kunz, S. Barth, A. Denker,* H. W. Drotleff,† J. W. Hammer, H. Knee,‡ and A. Mayer
Institut für Strahlenphysik der Universität Stuttgart, Germany
(Received 10 October 1995)

In a neutron-rich, α-rich environment that could arise during a supernova explosion the reaction chain $^{4}He(\alpha n,\gamma)^{9}Be(\alpha,n)^{12}C$ dominates the creation of carbon, which leads to the creation of heavier elements in the subsequent *r* process [S. E. Woosley and R. D. Hoffman, Astrophys. J. **395**, 202 (1992); B. S. Meyer, G. J. Matthews, W. M. Howard, S. G. Woosley, and R. D. Hoffman, *ibid.* **399**, 656 (1992); W. M. Howard, S. Goriely, M. Rayet, and M. Arnould, *ibid.* **417**, 713 (1993)]. For this reason the excitation function of the reaction $^{9}Be(\alpha,n)^{12}C$ has been measured in the energy range from $E_{\alpha}=366$ keV up to 3552 keV (corresponding $E_{\mathrm{c.m.}}=254-2450$ keV in the center-of-mass system) to obtain consistent data in the whole range, which were lacking in the literature. The measurements have been performed with a 4π detector and the yield contributions of the n_0 and n_1 neutron group could be resolved. Solid metallic targets of thickness 430 Å (7.75 $\mu g/cm^2$) and 650 Å (11.72 $\mu g/cm^2$) were used. Reaction rates and an analytic expression for them have been evaluated for $0.001 \leq T_9 \leq 10$. [S0556-2813(96)03205-0]

PACS number(s): 25.55.Hp, 26.30.+k, 27.20.+n

I. ASTROPHYSICAL SIGNIFICANCE

In the scenario for the *r* process proposed by Woosley and Hoffman [1], the reaction $^{9}Be(\alpha,n)^{12}C$ may play a dominant role as a linkage to the creation of ^{12}C. In a type-II supernova a so-called hot bubble is created between the emitted shell and the collapsing core. The material in this bubble is heated by neutrinos, which escape from the remaining core. A region of low density and high temperature[1] ($T_9 \approx 10$) is generated. Due to the high temperatures the heavier nuclei break up into neutrons and protons. With the expansion of the shell and of the hot bubble, the temperatures are dropping. At $T_9 \simeq 6$ the protons and neutrons start to recombine into α particles, and further to ^{12}C. This happens either by the triple-α process or by the neutron catalyzed reaction chain $^{4}He(\alpha n,\gamma)^{9}Be(\alpha,n)^{12}C$. In a neutron-rich environment the creation of ^{12}C by the reaction $^{4}He(\alpha n,\gamma)^{9}Be(\alpha,n)^{12}C$ is favored by a factor of approximately 10 compared with the triple-α process. ^{12}C again is the seed nucleus for the creation of heavier nuclei by fusion reactions with charged particles.

If the temperature drops below $T_9 \simeq 3$ the charged particle reactions start to freeze out. This freeze out stops at $T_9 \simeq 2$. The nuclei that have been built up to this moment are the seed nuclei for the succeeding *r* process. The described preceding process for the *r* process is called α-rich freezeout or neutron-rich α-rich freezeout, depending on a neutron-rich environment. In this process elements up to a mass of about $A \simeq 80$ are created. In the succeeding *r* process heavier elements are produced by neutron capture.

Because the creation of ^{12}C is only possible by the triple-α process or by the reaction $^{4}He(\alpha n,\gamma)^{9}Be(\alpha,n)^{12}C$, it is necessary to get exact knowledge of the reaction rates of both involved reactions in the temperature range of about $1 \leq T_9 \leq 6$.

II. EXPERIMENTAL SETUP

The measurements have been performed at the 4 MV-DYNAMITRON accelerator of the Institut für Strahlenphysik at Stuttgart in the context of a diploma thesis [2–5]. The reaction $^{9}Be(\alpha,n)^{12}C$ has been examined in the whole energy range from 366 up to 3552 keV (in the laboratory system), the range being determined by the energy range of the DYNAMITRON. In the $^{9}Be(\alpha,n)^{12}C$ reaction only very moderate He^{+} currents have been requested due to the rather high neutron yield. These for our accelerator small currents in the range of 30 nA to 3 μA have been measured by a very sensitive electrometer (Keithley model 617) with good common mode ripple suppression. The converted signal has been digitized by an Ithaco 385 analogue to digital converter.

The beam energy has been adjusted by a 90° magnetic analyzer, which has been calibrated using graphite targets and a narrow resonance at $E_{\alpha}=$ 1056.3 keV of the reaction $^{13}C(\alpha,n)^{16}O$ (data from the Ajzenberg compilation [6]). Furthermore two resonances at the laboratory energies 1336.7 keV and 1340.6 keV have also been used for the calibration.

The beryllium targets for the actual measurements were solid metallic targets. The beryllium has been evaporated on a copper backing using a protected evaporation facility. During evaporation the target thickness has been controlled with a quartz oscillator. For the experiments Be targets of thicknesses 5.18×10^{17} atoms/cm^2 (430 Å) and 7.83×10^{17} atoms/cm^2 (650 Å) have been used. The exact determination of the target thickness has been done using the narrow resonance at $E_{\alpha,\mathrm{lab}}=620$keV. The thickness of the targets correspond to an energy loss of the α particles of 13.8 keV and 20.8 keV at $E_{\alpha}=600$ keV.

The neutrons were detected by a 4π detector of high ef-

*Now at Hahn-Meitner-Institut, Berlin, Germany.
†Now at Technischer Überwachungsverein Hannover–Sachsen-Anhalt e.V., Hannover, Germany.
‡Now at Sligos Industries, Stuttgart, Germany.
[1] T_9 denotes the temperature in 10^9 K.

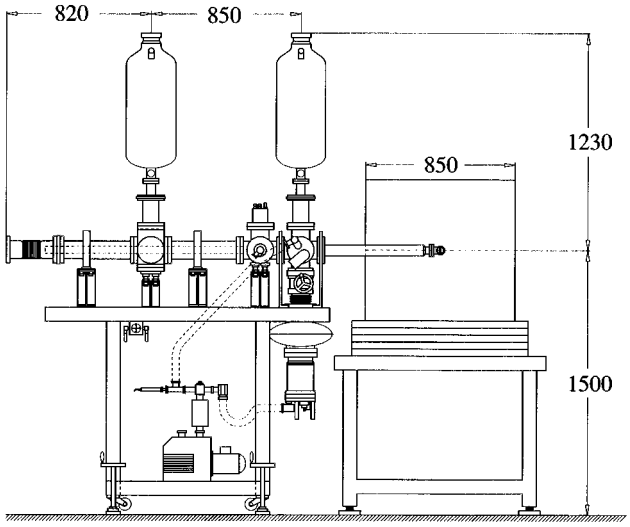

FIG. 1. Setup of the experiment for the measurement of ^{9}Be $(\alpha,n)^{12}$C. The beam line in front of the water-cooled Be target was equipped with two long copper tubes held at LN_2 temperature to prevent any target contamination. The turbomolecular pump was also used together with a LN_2 cryotrap to improve the vacuum to about 2×10^{-8} mbar with the beam on the target. On the right side the target is surrounded by the 4π neutron detector which is shown in detail in Fig. 2. All measures are given in mm.

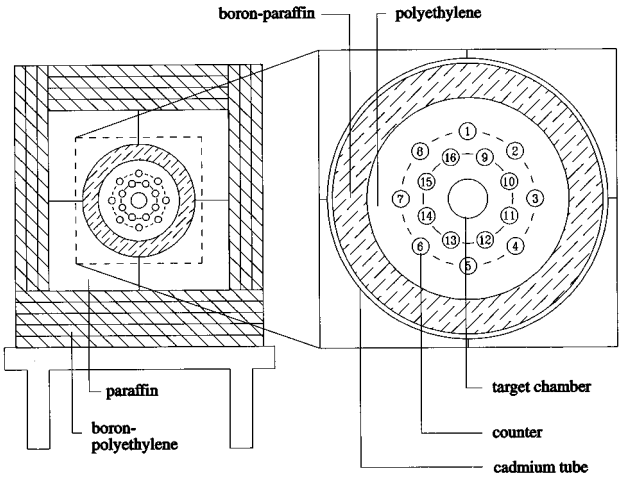

FIG. 2. Cross section of the 4π neutron detector. The projectiles are incidenting perpendicular to the shown plane along the axis of the target chamber. Around the target chamber the ^{3}He-filled proportional counters are located in two concentric rings in a distance of 8 cm and 12 cm from the axis of the target chamber to the center of a ^{3}He counter. Each counter is 2.5 cm in diameter and 50 cm long. The counters are embedded in a cylindrical polyethylene moderator of 35 cm diameter. In the outer parts the detector is shielded by layers of boron paraffin, boron polyethylene and cadmium. The cadmium tube has a diameter of 50 cm.

ficiency, which is described in more detail by Drotleff [7].

The target backings were water-cooled and were located at the end of a vacuum recipient with very clean conditions (Fig. 1). The targets have been similar to those used and described in a polarized neutron scattering experiment [8,9]. The vacuum was provided by a turbomolecular pump with a large LN_2 cryotrap in front of it. The beam tube was equipped with two long copper tubes held at liquid nitrogen temperature to prevent all carbon build up on the target surface. The beam was guided through three apertures preventing any deviation from the central position at the target. The vacuum in the last section of the beam line could be kept at 2×10^{-8} mbar with the beam on the target.

III. NEUTRON DETECTION

For neutron detection a special designed 4π detector [10] (Fig. 2) has been used. This detector consists of a cylindrical polyethylene moderator and a matrix of 16 ^{3}He-filled proportional counters. These counters are placed in two concentric rings around the target chamber, with each ring consisting of 8 counters. The distances from the axis of the target chamber to the counter rings were 8 cm and 12 cm, respectively. This configuration of the detector leads to a large efficiency of up to 38%, which is due to the moderator mass, the small distances between the counters and the target, and the large number of passes of the neutrons through the counters due to neutron diffusion, combined with rather low absorption in the moderator.

The efficiency of the detector in dependence of the neutron energy has been determined by Monte Carlo simulations using the code MCNP [11]. The resulting curve is shown in Fig. 3. These calculations have been tested by efficiency measurements with a calibrated ^{252}Cf-neutron source and some other nuclear reactions. These tests resulted in a good agreement of better than 3% relative deviation between measurement and simulation. The uncertainty assigned to the efficiency was less than 5%, depending on the neutron energy.

In the energy range of our measurements three possible neutron groups of the reaction ^{9}Be$(\alpha,n)^{12}$C can be released with Q values of $Q_0 = 5.704$ MeV, $Q_1 = 1.265$ MeV, and $Q_2 = -1.949$ MeV. Because of the negative Q value a threshold of $E_s = 2.8$ MeV exists for neutrons of the n_2 group. Van der Zwan and Geiger [12] showed that the yield contribution of the n_2 group is rather small for energies $E_{\alpha,\mathrm{lab}} < 3.7$ MeV, therefore this n_2 group was not considered in this investigation.

With the 4π detector a rough energy determination of the neutron energies could be performed making use of the energy dependence of neutron diffusion. The count rate ratio of the inner ^{3}He detectors to the outer ^{3}He detectors has a significant energy dependence sufficient for resolving the neutron groups of the ^{9}Be$(\alpha,n)^{12}$C reaction, because the energy of the two groups is in principle well separated due to the difference in the Q value, but it is smeared out according to reaction kinematics.

The efficiency $\varepsilon(Q,E)$ for neutrons of a neutron group with the Q value Q in dependence of the α energy E could be obtained by the relation

$$\varepsilon(Q,E) = \int\int d\Omega\, \varepsilon_n[E_n(Q,E,\theta)]P(Q,E,\theta). \qquad (1)$$

Here $\varepsilon_n(E_n)$ is the efficiency in dependence of the neutron energy and $E_n(Q,E,\theta)$ is the neutron energy for neutrons emitted with an angle θ, if the incidenting α particle had an energy E. This neutron energy is given solely by reaction kinematics [13]. $P(Q,E,\theta)$ is the angular distribu-

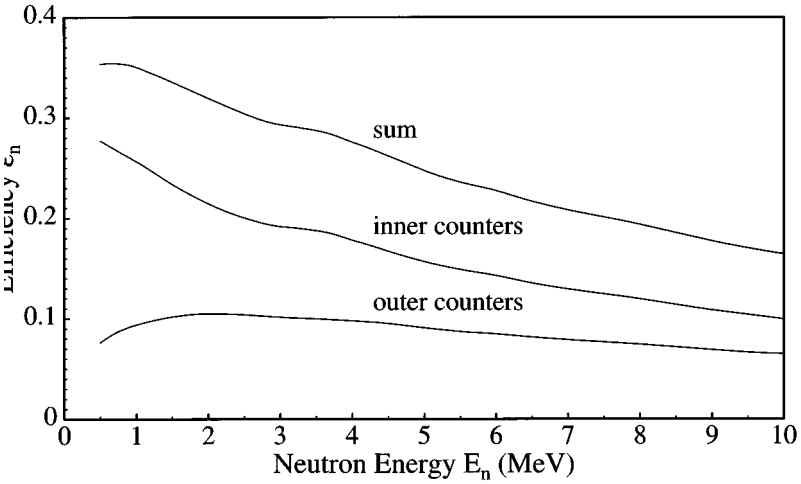

FIG. 3. Energy dependence of the efficiency ε_n of the two counter rings separate and as sum for neutron energies from 0.5 to 10 MeV.

tion for these neutrons and it could be obtained from the distribution in the center-of-mass system by the transformation $P(Q,E,\theta)=P_{\text{c.m.}}(Q,E_{\text{c.m.}},\theta_{\text{c.m.}})I_{\text{kin}}(Q,E,\theta)$, where $I_{\text{kin}}(Q,E,\theta)$ is also completely determined by reaction kinematics [13]. The angular distribution in the center-of-mass system was assumed to be isotropic. The possible error resulting from this assumption was tested using some angular distributions from literature [14,15] and it proved to be less than 0.5%.

The resulting experimentally determined yield for one neutron group is

$$Y_{\text{expt}}(E_\alpha,t)=\int_0^t dx n\sigma[E(x,E_\alpha)]\varepsilon[Q,E(x,E_\alpha)] \quad (2)$$

if straggling effects and the energy spread caused by the accelerator ripple are neglected. Here t is the thickness of the target, n is the number of target atoms per volume unit, σ the cross section and $E(x,E_\alpha)$ the energy of the projectiles at the depth x in the target, decreasing due to energy loss. E_α is the energy of the projectiles at $x=0$ on the target surface. This energy loss is described by the use of the stopping power ϵ:

$$\frac{dE(x,E_\alpha)}{dx}=-n\epsilon(E),$$

$$E(0,E_\alpha)=E_\alpha. \quad (3)$$

Here $\epsilon(E)$ denotes the energy loss dE in a layer of ndx target atoms per cm^2. This function is obtained from the tables of Ziegler [16]. For the target thicknesses used in this experiment ($\Delta E<25$ keV), Eq. (3) can be approximated by

$$E(x,E_\alpha)\simeq E_\alpha-\epsilon(E)nx. \quad (4)$$

Normally the thickness of the target is small enough to treat the efficiency $\varepsilon[Q,E(x,E_\alpha)]$ as constant within the integration interval and in this experiment the relative variation is less than 0.3%.

If one distinguished both neutron groups n_0 and n_1 and if one makes use of the two counter rings of the detector, the measured neutron yield could be obtained by

$$Y_{\text{inn}}(E_\alpha)=\varepsilon_{\text{inn}}(Q_0,E_\alpha)Y_0(E_\alpha)+\varepsilon_{\text{inn}}(Q_1,E_\alpha)Y_1(E_\alpha)+Y_{\text{back, inn}}(E_\alpha), \quad (5)$$

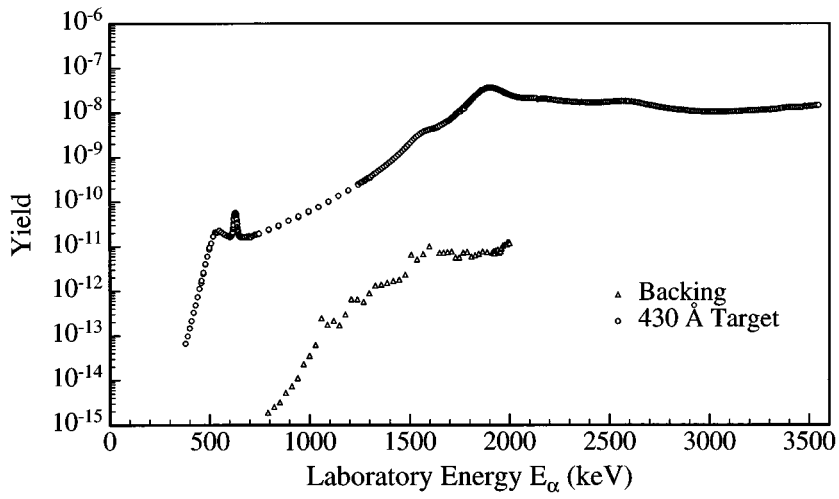

FIG. 4. Yield curve for the reaction $^9\text{Be}(\alpha,n)^{12}\text{C}$ in comparison with a pure copper backing. Because the $^9\text{Be}(\alpha,n)^{12}\text{C}$ yield is several orders of magnitude larger than the yield from the backing, neutrons arising from background reactions could be neglected.

$$Y_{\text{out}}(E_\alpha)=\varepsilon_{\text{out}}(Q_0,E_\alpha)Y_0(E_\alpha)+\varepsilon_{\text{out}}(Q_1,E_\alpha)Y_1(E_\alpha)+Y_{\text{back, out}}(E_\alpha).$$

Here the indices inn and out indicate the inner and outer counter rings. Y_i is the yield for neutrons of the group n_i, $\varepsilon_{\text{ring}}$ is the efficiency in the corresponding counter ring, Y_{ring} is the measured yield and $Y_{\text{back, ring}}$ is the contribution of the background to the measured yield.

The efficiencies ε_{inn} and ε_{out} have been calculated via Monte Carlo simulations and according to Eq. (1), and the yield Y_{inn} and Y_{out} has been measured. If the yield $Y_{\text{back, inn}}$ and $Y_{\text{back, out}}$ has also been measured or could be neglected as in the case of the ^{9}Be$(\alpha,n)^{12}$C reaction (Fig. 4), equation system (5) can be solved to obtain the yield Y_0 and Y_1 for the two neutron groups. The total yield is then

$$Y=Y_0+Y_1. \tag{6}$$

IV. EXCITATION FUNCTION AND *S* FACTOR

The connection between the cross section and the total yield is given by the equation

$$Y(E_\alpha)=\int_0^t dx n\sigma[E(x,E_\alpha)]. \tag{7}$$

The astrophysical S factor is introduced to separate the energy dependence of the Coulomb barrier penetration from the cross section and it is obtained by

$$S(E)=\sigma(E)E\exp(2\pi\eta)=\sigma(E)E\exp\left(\sqrt{\frac{E_G}{E}}\right), \tag{8}$$

where

$$E_G=\left(\frac{e^2}{2\varepsilon_0\hbar}Z_1Z_2\right)^2\frac{\mu}{2} \tag{9}$$

is the Gamow energy and

$$\eta=\frac{Z_1Z_2e^2}{4\pi\varepsilon_0\hbar}\sqrt{\frac{\mu}{2E}} \tag{10}$$

is the Sommerfeld parameter. Z_1 and Z_2 are the nuclear charges of the target and projectile nuclei and μ is the reduced mass. The energy E has to be taken in the center-of-mass system.

If the variation of the cross section in the energy range given by the energy loss of the projectiles in the target could be neglected, Eq. (7) could simply be written as

$$Y(E_\alpha)=nt\sigma(E_{\alpha,\text{eff}}), \tag{11}$$

where $E_{\alpha,\text{eff}}$ is the effective energy of the projectiles in the target. In a first approach $E_{\alpha,\text{eff}}$ can be written as $E_{\alpha,\text{eff}}\simeq E_\alpha-\Delta E/2$, were ΔE is the target thickness.

The Breit-Wigner formula has been applied to the resonant cross section:

$$\sigma_{\text{res}}(E)=\pi\lambda^2\omega\gamma\frac{\Gamma}{(E-E_R)^2+(\Gamma/2)^2}, \tag{12}$$

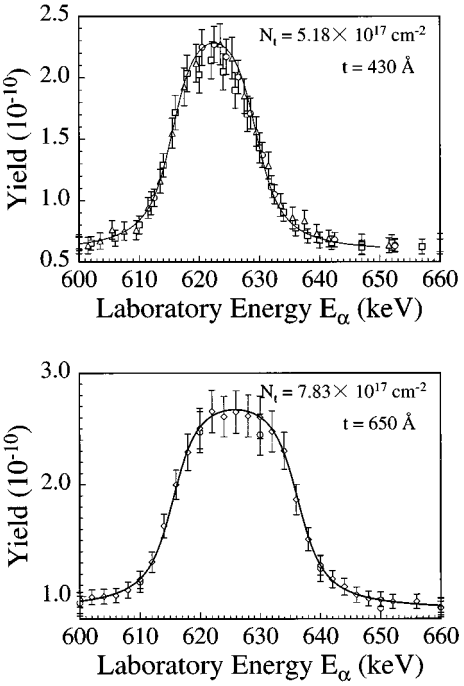

FIG. 5. Yield for the resonance at $E_{\alpha,\text{lab}}=620$ keV ($E_{\text{c.m.}}=429$ keV) for both targets. The solid line is a fit for the thick-target yield. The various symbols for the data points indicate different runs in the experiment.

$$\lambda^2=\frac{\hbar^2}{2\mu E_{\text{c.m.}}},\qquad \omega\gamma=\omega\frac{\Gamma_\alpha\Gamma_n}{\Gamma}. \tag{13}$$

Here $\omega\gamma$ denotes the strength, Γ the total width, Γ_α and Γ_n the partial widths of the resonance. As an approximation the energy dependence of the partial α-width in the entrance channel is $\Gamma_\alpha\propto\exp(-\sqrt{E_G/E})$. If the energy dependence of the partial width of the neutron channel and the total width are neglected, a resonance is described with respect to the S-factor function by the formulas

$$S_{\text{res}}(E)=S_R\frac{(\Gamma/2)^2}{(E-E_R)^2+(\Gamma/2)^2}, \tag{14}$$

$$S_R=\frac{2\pi\hbar^2}{\mu}\frac{(\omega\gamma)_R}{\Gamma_R}\exp\left(\sqrt{\frac{E_G}{E_R}}\right). \tag{15}$$

From the thick-target yield for the only narrow resonance at $E_{\alpha,\text{lab}}=620$ keV the determination of the target thickness is possible. The measured yield and the fitted thick-target yield for this resonance for both targets is shown in Fig. 5.

All other resonances of the reaction ^{9}Be$(\alpha,n)^{12}$C are broad in comparison with the energy loss of the α particles in the target, so the yield expression for a thin target from Eq. (11) could be applied. The resulting excitation functions for the two neutron groups are shown in Fig. 6, the total cross section is shown in Figs. 7 and 8 in different scales.

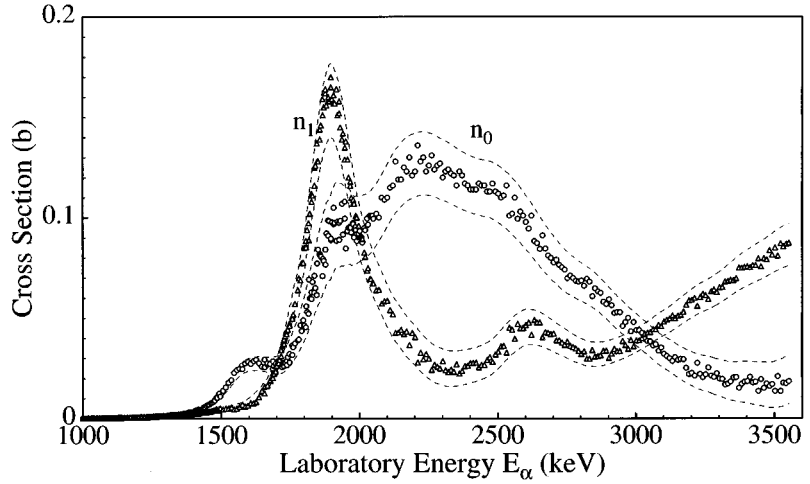

FIG. 6. Excitation function of ^{9}Be(α,n)^{12}C for the two neutron groups n_0 and n_1 in the energy range 1–3.5 MeV. The indicated band shows the region of uncertainty.

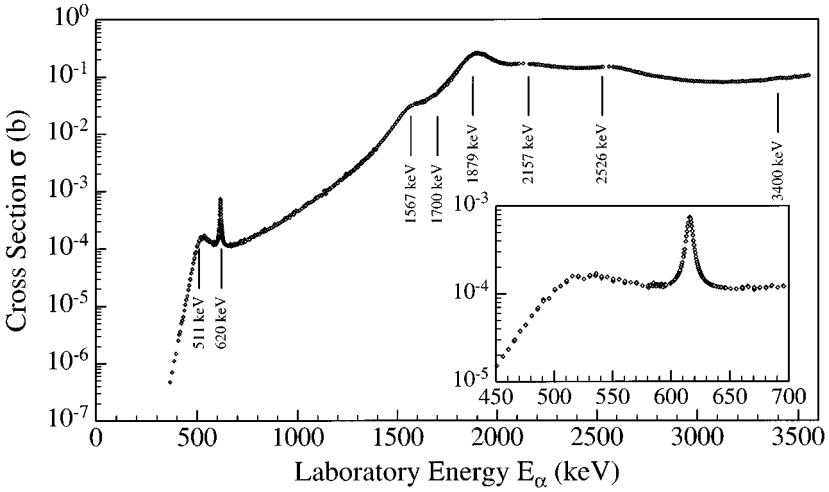

FIG. 7. Excitation function of the reaction ^{9}Be(α,n)^{12}C in the energy range of this experiment (366–3552 keV), for the sum of both neutron groups n_0 and n_1 in a logarithmic scale. The uncertainty of the experimental data is well below 15%. In the inserted window the part around the 620 keV resonance is shown enlarged.

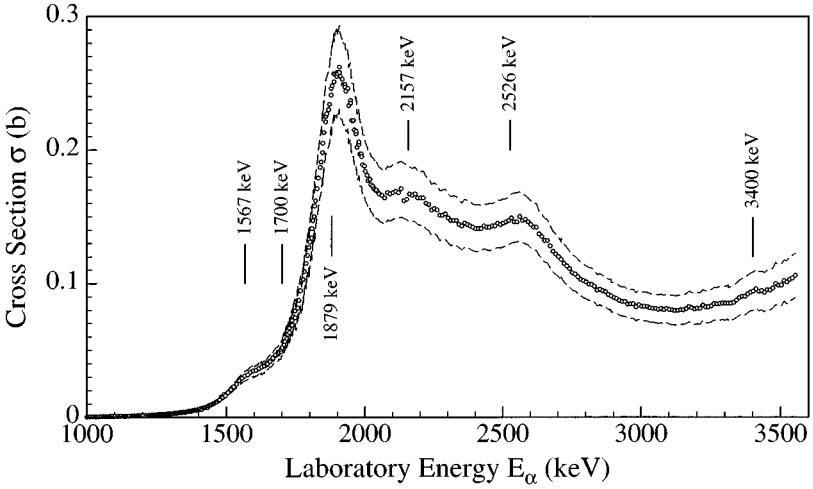

FIG. 8. Total cross section in linear representation, so that the resonances in the upper energy region are visible more clearly.

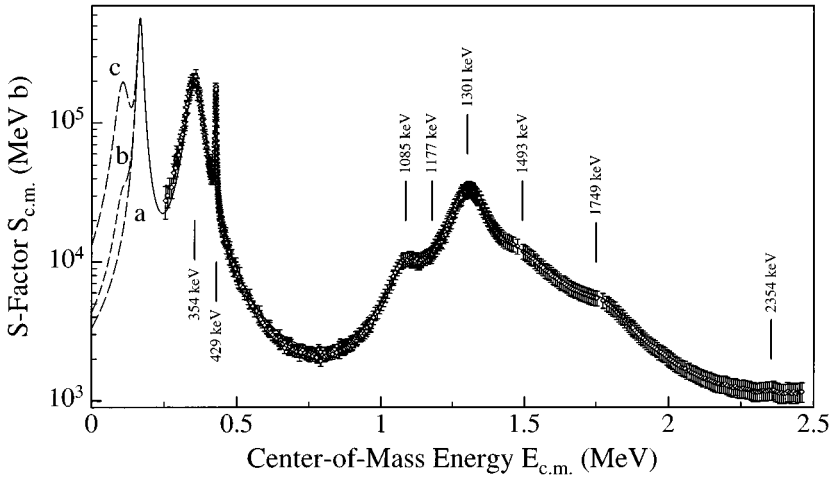

FIG. 9. S factor for the reaction ^{9}Be(α,n)^{12}C in the energy range of this experiment on a logarithmic scale. For energies below $E_{c.m.}=254$ keV the extrapolations towards lower energies are shown. At $E_{c.m.}=166$ keV a known resonance [18] is included. Because of a state in the compound nucleus a further resonance at $E_{c.m.}=106$ keV has to be taken into consideration. The curves shown are related to three cases: (a) no resonance at 106 keV, (b) the maximal possible strength multiplied by 0.1, estimated as described in the text, and (c) the maximal possible strength to obtain an upper limit.

The two resonances at $E_{\alpha,lab}=511$ keV and 620 keV are given enlarged as an inset of Fig. 7. The resulting S-factor curve is plotted in Fig. 9.

V. RESONANCE PARAMETERS

The resonance parameters have been determined by applying a sum of Breit-Wigner resonances as in Eq. (14) to the S-factor curve:

$$S(E)=\sum_J S_j \frac{(\Gamma_j/2)^2}{(E-E_j)^2+(\Gamma_j/2)^2}. \tag{16}$$

The use of a Breit-Wigner formula with constant Γ_j in the S factor corresponds to the consideration of an approximation of the energy dependence of the partial widths in the cross section σ, as described in the previous section.

This function has been converted to the reaction yield using Eqs. (8) and (7), which leads to

$$Y(E_\alpha,t)=\int_0^t dx n \frac{S(E)}{E}\exp\left(-\sqrt{\frac{E_G}{E}}\right). \tag{17}$$

Finally this expression was fitted to the experimentally determined yield, where E was evaluated from Eq. (3) by numerical integration. The resonance strength $(\omega\gamma)_j$ has been obtained from S_j by Eq. (15).

The resonances in the upper energy region have been fitted with the assumption that only the resonances given in Table I are contributing to the cross section. But in this region further states in the compound nucleus are known, so that one has to consider contributions from these states.

At $E_{\alpha,lab}\simeq 3400$ keV ($E_{c.m.}\simeq 2354$ keV) a small bump in the cross section (Figs. 7 and 8) and in the S factor (Fig. 9) has been detected. At the corresponding excitation energy of $E_x=13$ MeV a state in the compound nucleus is known [17]. But this resonance is so small that numerical evaluation is not possible.

At $E_{\alpha,lab}\simeq 1700$ keV ($E_{c.m.}\simeq 1177$ keV) a shoulder is showing up between the two surrounding resonances (Figs. 7–9). Because of a state in the compound nucleus at $E_x=11.83$ MeV [17] this shoulder was assigned to the resonance. For this resonance the parameters could not be evaluated with a reasonable error.

Compared with previous publications of our experiment [2–4] the resonance parameters have changed, due to the different way of their determination. Previously Eq. (12) was used directly in the cross section data, neglecting all energy

TABLE I. Resonance parameters in the center-of-mass system for the reaction ^{9}Be(α,n)^{12}C obtained by this experiment. All parameters have been determined by fitting Eq. (16) to the measured yield. The strength $(\omega\gamma)_{c.m.}$ has been determined from $S_{R,c.m.}$ using Eq. (15). The last column shows the excitation energy E_x from the Ajzenberg compilation [17] that was assigned to the measured resonances.

Energy		Width	Strength		^{13}C*
$E_{\alpha,lab}$ (keV)	$E_{c.m.}$ (keV)	$\Gamma_{c.m.}$ (keV)	$S_{R,c.m.}$ (MeV b)	$(\omega\gamma)_{c.m.}$ (eV)	E_x (MeV)
511 ± 7	354 ± 5	56 ± 5	$(2.0\pm0.3)\times10^5$	2.86 ± 1.00	10.996
620 ± 4	429 ± 3	< 4.8	$(1.4\pm0.3)\times10^5$	1.31 ± 0.34	11.080
1567 ± 22	1085 ± 15	122 ± 20	$(6.5\pm1.5)\times10^3$	2700 ± 900	11.748
≈ 1700	≈ 1177		—	—	11.848
1879 ± 7	1301 ± 5	150 ± 13	$(3.3\pm0.4)\times10^4$	50 300 ± 8000	11.950
2157 ± 29	1493 ± 20	243 ± 40	$(6.9\pm1.0)\times10^3$	36 800 ± 9 700	12.140
2526 ± 29	1749 ± 20	336 ± 50	$(3.5\pm0.6)\times10^3$	58 500 ± 1 500	12.438
≈ 3400	≈ 2354	—	—	—	13.000

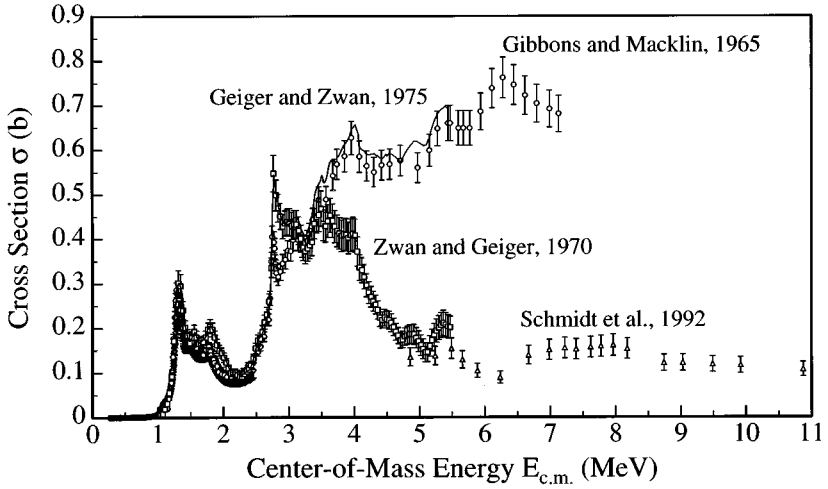

FIG. 10. Extension of the excitation function of $^{9}\mathrm{Be}(\alpha,n)^{12}\mathrm{C}$ for energies up to $E_{\mathrm{c.m.}}=11$ MeV. The data of Gibbons and Macklin [22] include neutrons from the breakup reaction, the data of Geiger and van der Zwan [23] include the neutron groups n_0 to n_3 and neutrons from the breakup reaction, the data of van der Zwan and Geiger [12] include the neutron groups n_0 to n_2 and the data of Schmidt *et al.* [15] include the neutron groups n_0 to n_6.

dependences of the partial widths. The use of the Breit-Wigner formula in the S factor corresponds to an approximation of the energy dependence of the partial α width as described above. From this the parameters given in Table I are derived. These parameters are only valid for the description of the measured data using the procedure mentioned above. Only the parameters for the narrow resonance at $E_{\alpha,\mathrm{lab}}=620$ keV are not strongly affected by different evaluation procedures.

Comparing our new data on the $^{9}\mathrm{Be}(\alpha,n)^{12}\mathrm{C}$ resonances (Table I) with data from literature, there is agreement in some cases but disagreement in others. For instance there is disagreement concerning the $E_{\alpha}=620$ keV resonance with the values given by Davids [14]: $E_{\alpha}=600$ keV and $(\omega\gamma)_{\mathrm{c.m.}}=0.88$ eV. In this investigation we detected weak resonances at $E_{\alpha}=1567$ keV and $E_{\alpha}=2157$ keV which are not listed in the Ajzenberg compilation [17]. However a resonance at $E_{\alpha}=2240$ keV reported by Ajzenberg could not be observed in this experiment. Due to the broad structures in the $^{9}\mathrm{Be}(\alpha,n)^{12}\mathrm{C}$ excitation function it cannot be excluded that some structures have to be assigned to more than one level in the compound nucleus.

VI. REACTION RATES

The reaction rate $N_A\langle\sigma v\rangle$ has been determined by numerical integration of the equation

$$N_A\langle\sigma v\rangle = N_A\left(\frac{8}{\pi\mu}\right)^{1/2}\frac{1}{(kT)^{3/2}}\int_0^{\infty} dE\,\sigma(E)E\exp\left(-\frac{E}{kT}\right) \tag{18}$$

so differences in the determination of the resonance parameters make no effect in the finally evaluated reaction rate. Because the integration has to be taken from energy zero up to ∞, the measured excitation function had to be extended to higher and lower energies.

For energies $E_{\mathrm{c.m.}}<254$ keV, which cannot be reached with our accelerator, the cross section was extrapolated with the tails of the observed resonances. At $E_{\mathrm{c.m.}}=166$ keV an additional resonance was taken into account, using the data of Wrean, Brune, and Kavanagh [18]. This resonance is approximately a factor of 10 stronger than assumed by Caughlan and Fowler for their calculation of the reaction rates [19]. Because of a known state in the compound nucleus at $E_x=10.753$ MeV [17] a further resonance has been assumed at $E_{\mathrm{c.m.}}=106$ keV. The strength of this resonance can be estimated using Eq. (13). The partial width of the neutron channel $\Gamma_{n,\mathrm{c.m.}}=(43.4\pm0.9)$ keV and the total width $\Gamma_{\mathrm{c.m.}}=(50.9\pm0.6)$ keV are given by Cierjacks *et al.* [20], the partial width $\Gamma_{\alpha,\mathrm{c.m.}}$ of the α channel could be estimated by

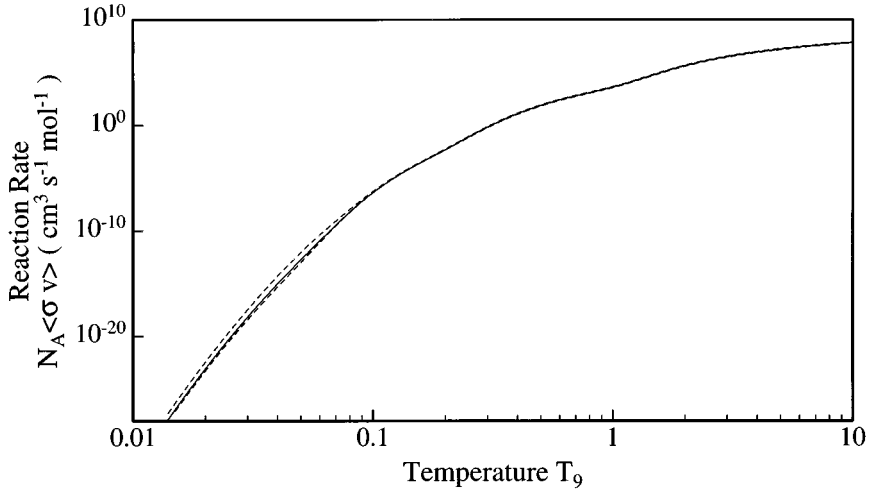

FIG. 11. Reaction rate for $^{9}\mathrm{Be}(\alpha,n)^{12}\mathrm{C}$ vs temperature T_9. The dashed curves indicate the band of uncertainty.

TABLE II. Coefficients for the analytical expression of the reaction rate.

C_0		C_1	C_2	C_3
4.56×10^{13}		8.3	580	0.363
i	1	2	3	4
A_i	5.1×10^{-6}	0.92	6×10^{6}	2.2×10^{8}
B_i	1.14	1.84	7.46	12.9

$$\Gamma_{\alpha,\mathrm{c.m.}}=\frac{2\hbar}{R_n}\sqrt{\frac{2E_{\mathrm{c.m.}}}{\mu}}\frac{1}{F_L(\eta,\rho)^2+G_L(\eta,\rho)^2}\theta_L^2 \quad (19)$$

as given by Rolfs and Rodney [21]. Here R_n is the nuclear radius, η is the Sommerfeld parameter given in Eq. (10), $\rho=R_n\sqrt{2\mu E_{\mathrm{c.m.}}/\hbar^2}$, L is the angular momentum of the α particle, $F_L(\eta,\rho)$ and $G_L(\eta,\rho)$ are the Coulomb wave functions and θ_L^2 is the reduced width with $\theta_L^2\leqslant1$. For the strength of this resonance we assumed three cases: (a) strength zero, (b) the maximal possible strength given in Eqs. (13) and (19) multiplied by 0.1, which is almost the value adopted by Caughlan and Fowler [19], and (c) the maximal possible strength. The resulting extensions for the S factor are shown in Fig. 9.

For $E_{\mathrm{c.m.}}>2.45$ MeV data of Gibbons and Macklin [22] and van der Zwan and Geiger [12,23,24] are available. Because Gibbons and Macklin could not distinguish neutron groups their yield included also neutrons from the breakup reaction $^9\mathrm{Be}(\alpha,\alpha')^9\mathrm{Be}^*\rightarrow{}^8\mathrm{Be}+n$, which contributes significantly to the neutron yield for $E_{\alpha,\mathrm{lab}}>4$ MeV [23]. So the Gibbons and Macklin cross section values are higher than that for the pure $^9\mathrm{Be}(\alpha,n)^{12}\mathrm{C}$ reaction. For this reason we used the data of van der Zwan and Geiger to cover the energies between the range of our data ($E_{\mathrm{c.m.}}=2.5$ MeV) and $E_{\mathrm{c.m.}}=4.86$ MeV. Between $E_{\mathrm{c.m.}}=4.86$ MeV and 10.87 MeV data of Schmidt *et al.* [15] have been used, for $E_{\mathrm{c.m.}}>10.87$ MeV the cross section was assumed to be constant, which seems to be reasonable from the general trend of the excitation function. This extension towards higher energies is shown in Fig. 10.

The uncertainty in the resulting reaction rate is less than 15% in the relevant temperature region. Consideration of the possible resonance at $E_{\mathrm{c.m.}}=106$ keV leads to an increase of the reaction rate and the uncertainty band, but only for low temperatures. The resulting reaction rate is plotted in Fig. 11.

To obtain an analytical expression the formula given in Eq. (20) was fitted to the numerical reaction rate data:

$$N_A\langle\sigma v\rangle=\frac{C_0}{T_9^{2/3}}\exp\left(-\frac{23.859}{T_9^{1/3}}-\left(\frac{T_9}{C_3}\right)^2\right)(1+0.017464T_9^{1/3}+0.68529C_1T_9^{2/3}+0.08377C_1T_9+0.23481C_2T_9^{4/3}$$
$$+0.072966C_2T_9^{5/3})+\sum_{i=1}^{3}\frac{A_i}{T_9^{3/2}}\exp\left(-\frac{B_i}{T_9}\right)+A_4\exp\left(-\frac{B_4}{T_9}\right). \quad (20)$$

The coefficients of this fit are given in Table II, and it is valid for $0.001\leqslant T_9\leqslant10$. In this region the difference between the fit and the numerical data is less than 10%. The single expressions in this fit look like resonant and nonresonant contributions, but all parameters have been allowed to vary during the fit, so the coefficients don't reflect any physical quantities.

VII. CONCLUSION

In comparison with the evaluation by Caughlan and Fowler [19] our rates agree within 50% for $T_9>0.3$. For lower temperatures our results are up to a factor of 10 higher than those of Caughlan and Fowler (Fig. 12). This is due to the resonance at $E_{\mathrm{c.m.}}=166$ keV, which has been underestimated by Caughlan and Fowler.

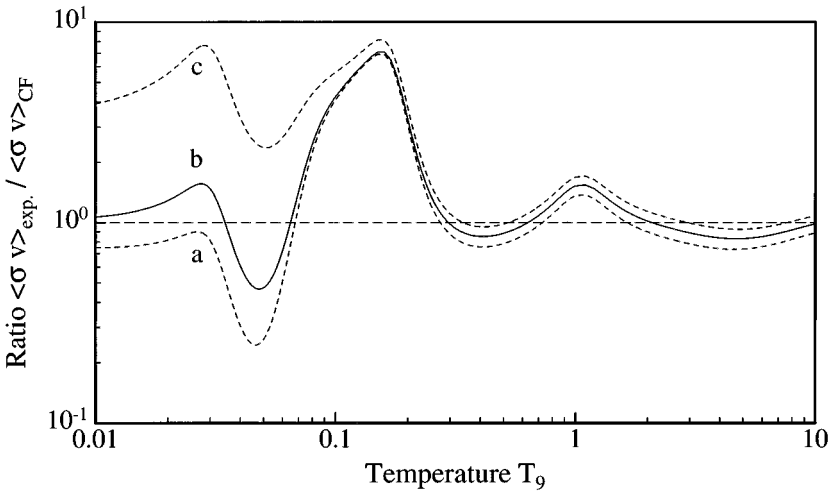

FIG. 12. Ratio of our reaction rate of ^{9}Be $(\alpha,n)^{12}$C compared to the compilation rate of Caughlan and Fowler [19]. The solid line is our final recommended rate, the dashed lines indicate the region of uncertainty. For higher temperatures this region is determined by the uncertainty in our measured cross section data and by the uncertainty of the additional data. Towards lower temperatures the area of uncertainty is determined by the extrapolation of the excitation function towards lower energies and especially the strength of the resonance at $E_{\mathrm{c.m.}}=106$ keV. The curves (a), (b) and (c) have the same meaning as in Fig. 9.

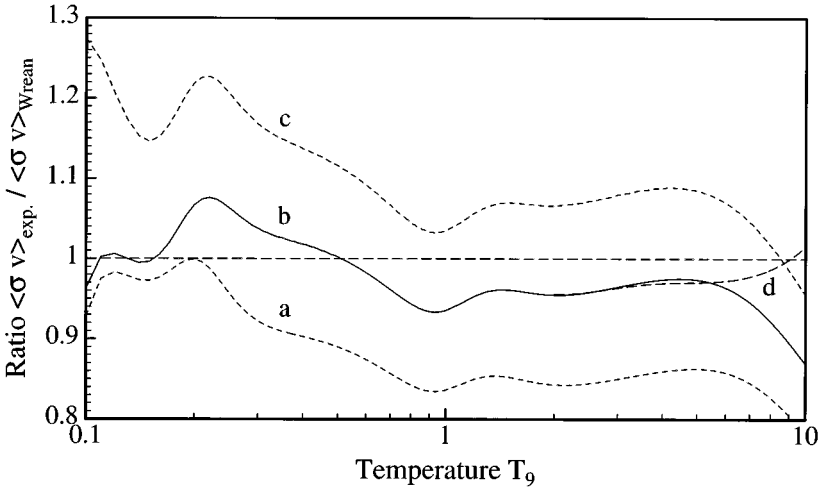

FIG. 13. Ratio of our reaction rate of ^{9}Be (α,n) ^{12}C compared to the rate of Wrean *et al.* [18]. The curves (a), (b), and (c) have the same meaning as in Figs. 9 and 12. Curve (d) displays the influence of the extension towards higher energies using the data of Gibbons and Macklin [22]. This curve has been added because Wrean *et al.* took the Gibbons and Macklin data for their extension towards higher energies. Both results agree excellent (within 10%, which is better than the uncertainty of the data).

Compared with the fit for the reaction rates of Wrean *et al.* [18] our rates fit within 10% for $T_9>0.1$, which is in the error range of both data sets (Fig. 13). For temperatures $T_9>6$ the difference is getting higher because Wrean *et al.* used for their extension towards higher energies the data of Gibbons and Macklin [22], which are too high for reasons given above.

In the temperature range of interest for the reaction chain ^{4}He$(\alpha n,\gamma)$ ^{9}Be(α,n) ^{12}C $(1\leqslant T_9\leqslant 6)$ the reaction rate is not affected by the low energy resonances at all and agrees reasonably with previous evaluations. Compared with the evaluation by Wrean *et al.* the agreement is excellent, so the reaction rate can be considered as fully evaluated.

ACKNOWLEDGMENTS

We would like to thank Prof. Dr. U. Kneißl for his interest and support. We are obliged to the DYNAMITRON crew (head H. Hollick) for providing the beam.

[1] S. E. Woosley and R. D. Hoffman, Astrophys. J. **395**, 202 (1992).
[2] R. Kunz, Diploma thesis, Stuttgart, 1993.
[3] R. Kunz, S. Barth, A. Denker, H. W. Drotleff, J. W. Hammer, H. Knee, and A. Mayer, in *Proceedings of the European Workshop on Heavy Element Nucleosynthesis*, edited by E. Somorjai and Z. Fülöp (Budapest, Hungary, 1994), pp. 134–139.
[4] R. Kunz, A. Denker, H. W. Drotleff, M. Große, H. Knee, S. Küchler, R. Seidel, M. Soiné, and J. W. Hammer, in *Proceedings of the 4th International Conference on Applications of Nuclear Techniques ''Neutrons and their Applications,''* Crete, Greece, edited by G. Vourvopoulos and T. Paradellis [Proc. SPIE **2339**, 33 (1995)].
[5] A. Denker, H. W. Drotleff, M. Große, H. Knee, R. Kunz, A. Mayer, R. Seidel, M. Soiné, and J. W. Hammer, in *Proceedings of the International Symposium on Nuclei in the Cosmos III, Assergi, Italy*, edited by M. Busso, R. Gallino, and C. M. Raiteri, AIP Conf. Proc. No. 327 (AIP, New York, 1995), pp. 225–258.
[6] F. Ajzenberg-Selove, Nucl. Phys. **A460**, 1 (1986).
[7] H. W. Drotleff, Ph.D. thesis, Bochum und Stuttgart, 1992.
[8] J. W. Hammer, G. Bulski, W. Grum, W. Kratschmer, H. Postner, and G. Schleussner, Nucl. Instrum. Methods A **244**, 455 (1986).
[9] W. Weiss, W. Grum, J. W. Hammer, M. Koch, and G. Schreder, Nucl. Instrum. Methods A **292**, 359 (1990).
[10] A. Denker, H. W. Drotleff, M.Große, J. W. Hammer, H. Knee, R. Kunz, A. Mayer, R. Seidel, and G. Wolf, in *Proceedings of the 7th Workshop on Nuclear Astrophysics, Ringberg Castle, Tegernsee, Germany*, edited by W. Hillebrandt and E. Müller (Max-Planck-Institut für Astrophysik, München, Germany, 1993), pp. 123–131.
[11] J. F. Briesmeister, MCNP, A General Monte Carlo *N*-Particle Transport Code, Version 4A, LA-12625-M, Los Alamos National Laboratory, 1993.
[12] L. van der Zwan and K. W. Geiger, Nucl. Phys. **A152**, 481 (1970).
[13] P. Marmier and E. Sheldon, *Physics of Nuclei and Particles* (Academic Press, New York, 1969).
[14] C. N. Davids, Nucl. Phys. **A110**, 619 (1968).
[15] D. Schmidt, R. Böttger, H. Klein, and R. Nolte, Physikalisch-Technische Bundesanstalt Braunschweig Report PTB-N-7 and Report PTB-N-8.
[16] J. F. Ziegler, *The Stopping and Ranges of Ions in Matter* (Pergamon Press, New York, 1977), Vol. 4.
[17] F. Ajzenberg-Selove, Nucl. Phys. **A523**, 1 (1991).
[18] P. R. Wrean, C. R. Brune, and R. W. Kavanagh, Phys. Rev. C **49**, 1205 (1994).
[19] G. R. Caughlan and W. A. Fowler, At. Data Nucl. Data Tables **40**, 283 (1988).
[20] S. Cierjacks, F. Hinterberger, G. Schmalz, D. Erbe, P. v. Rossen, and B. Leugers, Nucl. Instrum. Methods **169**, 185 (1979).

[21] C. E. Rolfs and W. S. Rodney, in *Cauldrons in the Cosmos*, edited by C. E. Rolfs (The University of Chicago Press, Chicago, 1988).

[22] J. H. Gibbons and R. L. Macklin, Phys. Rev. B **137**, 1508 (1965).

[23] K. W. Geiger and L. van der Zwan, Nucl. Instrum. Methods **131**, 315 (1975).

[24] K. W. Geiger and L. van der Zwan, National Research Council Canada Report NRCC-15303.